DYNAMIC ANALYSIS OF A FAST RESPONSE, AIR-TO-FUEL EQUIVALENCE RATIO SENSOR

Michael J. Brear
Department of Mechanical and Manufacturing Engineering
University of Melbourne, Australia
mjbrear@unimelb.edu.au

Malcolm Jones
Department of Mechanical and Manufacturing Engineering
University of Melbourne, Australia
mbjones@mame.mu.oz.au

ABSTRACT

Guibert & Dicocco have recently designed and tested a sensor for measuring the equivalence ratio of a mixture of hydrocarbon fuel and air. Since this sensor utilised the operating principles of constant temperature, hot-wire anemometry, it is in principle capable of a fast dynamic response even though Guibert & Dicocco only verified the sensor's function at low frequencies. This paper therefore intends to develop further the ideas of Guibert & Dicocco by proposing quasi-analytic transfer functions that govern the sensor's dynamic performance. Classical control techniques are then used to examine the frequency response, stability and the sensitivity of various sensor designs.

INTRODUCTION

Numerous engineering devices utilise the combustion of hydrocarbons for the production of mechanical energy. Most of these systems, such as automotive engines or gas turbines, feature important combustion phenomena with short time scales. In order to observe these phenomena, a fast response sensor for the measurement of air-to-fuel equivalence ratio is highly desirable.

Guibert & Dicocco [1] have recently designed and tested one such sensor for the measurement of the equivalence ratio of a mixture of hydrocarbons and air. As Figure 1 shows, their sensor consists of a choked sampling tube which heats the air fuel mixture to a constant temperature prior to the mixture passing over a Platinum/Iridium hot-wire. The throat and the heating element therefore remove the sensitivity of the hot-wire to fluctuations in velocity and temperature.

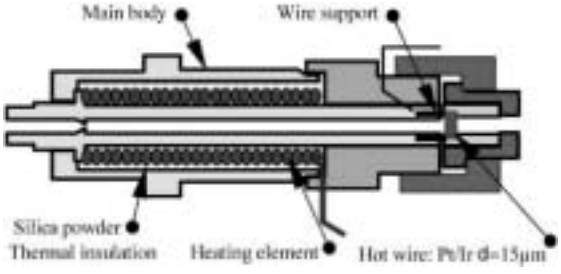

Figure 1: Schematic sectional diagram of Guibert & Dicocco's [3] sensor (from [3])

This sensor utilises the operating principles of constant temperature anemometry (CTA) with hot-wires, but with several significant differences. In the case of CTA, the electrical input to the hot-wire is intended to balance only the convective loss of energy from the wire to the passing fluid. Thus, the voltage over the wire is related to the fluid velocity. With Guibert & Dicocco's equivalence ratio sensor, the hot-wire is made from a catalytic material and is heated to a temperature above the ignition temperature of the fuel/air mixture. The wire therefore causes the mixture surrounding it to react and release energy to the wire. As Guibert & Dicocco show, the voltage across the wire is then related to the local air/fuel equivalence ratio around the wire.

However, Guibert & Dicocco only verified the function of their sensor for low frequencies. This paper is therefore intended to develop further the ideas of Guibert & Dicocco by proposing quasi-analytic relationships that govern the sensor's dynamic performance. Linear theory that is based on that presented in Perry [7] for CTA is used to derive the transfer function between the local equivalence ratio surrounding the wire and the wire voltage. Using Perry's [7] bridge circuit and related electronics, the transfer function between the equivalence ratio and the bridge output voltage is then determined. When incorporated into the bridge, the bandwidth of the sensor is similar to usual CTA configurations, but with added effects due to the mass transfer and catalysis. Including these additional parameters, classical control techniques are then used to determine the optimal frequency response and sensitivity of various configurations.

NOMENCLATURE

A_w wire surface area (m^2)
a sensitivity of hot-wire's resistance to temperature variations ($1/K$)
C_g hydrocarbon concentration in the gas (mol/m^3)
C_w hydrocarbon concentration on the wire surface (mol/m^3)

c specific heat capacity of hot-wire (J/m^3K)
D_h hydrocarbon diffusion coefficient (m^2/s)
d_w wire diameter (m)
E_w hot-wire voltage (V)
e_w hot-wire voltage perturbation (V)
E_0 bridge output voltage (V)
e_0 bridge output perturbation voltage (V)
h heat transfer coefficient (W/m^2K)
h_m mass transfer coefficient (m/s)
I current through hot-wire (A)
i hot-wire current perturbation (A)
k thermal conductivity of hot-wire (W/mK)
k_1 constant
l_w hot-wire length (m)
Nu Nusselt number based on hot-wire diameter
P_J Joule heating of hot-wire (W)
P_A accumulation of heat within the hot-wire (W)
P_R power generated by the catalysis (W)
P_T energy lost by forced convection (W)
Pr Prandtl number
R_g hot-wire resistance at the gas temp. (Ω)
R_w hot-wire resistance at the operating temp. (Ω)
R_0 hot-wire resistance at the reference temp. (Ω)
Re Reynolds number based on hot-wire diameter
Sh Sherwood number
s Laplace transform variable
T_g gas temperature (K)
T_w hot-wire temperature (K)
T_w hot-wire time constant (K)
T_0 reference temperature ($273.15K$)
t time (s)
U gas velocity (m/s)
$\overline{U}$ mean gas velocity (m/s)
u' velocity perturbation (m/s)
V hot-wire volume (m^3)
X constant
Y constant
y constant
α constant
β constant
χ molar fraction of hydrocarbon (mol/kg)
ϕ air-to-fuel equivalence ratio
$\overline{\phi}$ mean equivalence ratio
ϕ' equivalence ratio perturbation
γ constant
ρ_g density of mixture (kg/m^3)
σ rate of hydrocarbon consumption per unit surface area (mol/m^2s)
ΔH enthalpy of reaction (J/mol)

THEORY

Problem formulation

Guibert & Dicocco's sensor functions by balancing the electrical energy into the hot-wire with the energy transferred to and from the fluid, such that the hot-wire is maintained at a roughly constant temperature. This can be expressed as

$$P_J + P_R = P_A + P_T \tag{1}$$

where P_R is zero for hot-wire anemometry [1, 7]. The Joule heating of the hot-wire is

$$P_J = I^2 R_w \tag{2}$$

and, modelling the hot-wire as a 'lumped body' of uniform temperature T_w, the accumulation of heat within the hot-wire is

$$P_A = cV\frac{dT_w}{dt}. \tag{3}$$

Perry [7] expresses the resistance of the hot-wire at temperature T_w in terms of a power series truncated to first order:

$$R_w = R_0\left[1 + a\left(T_w - T_0\right)\right]. \tag{4}$$

Defining the resistance of the hot-wire at the gas temperature T_g similarly, it follows that

$$R_w - R_g = aR_0\left(T_w - T_g\right), \tag{5}$$

which, combined with equation (3), gives

$$P_A = k_1\frac{dR_w}{dt}. \tag{6}$$

where

$$k_1 = \frac{cV}{aR_0}.$$

Newton's law of cooling states that

$$P_T = hA_w\left(T_w - T_g\right). \tag{7}$$

By combining Kramers' [6] empirical law for the forced convection from an infinitely long, straight circular cylinder in a cross-flow:

$$Nu = 0.42Pr^{0.2} + 0.57Pr^{0.33}\sqrt{Re}, \tag{8}$$

with equation (5), Perry [7] expresses the convective heat loss as

$$P_T = \left(R_w - R_g\right)F\left(U\right) \tag{9}$$

with $F\left(U\right)$ defined as

$$F\left(U\right) = X + Y\sqrt{U}$$

with constants

$$X = 0.42\frac{A_S k}{R_0 a d_w}Pr^{0.2}$$

and

$$Y = 0.57\frac{A_S k}{R_0 a d_w}Pr^{0.33}\left(\frac{\rho_g d_w}{\mu_g}\right)^{0.5}.$$

Power generated by catalysis

The sensor studied by Guibert & Dicocco [3] exploits a catalytic reaction on the hot-wire surface, which releases its enthalpy of reaction into the hot-

wire. By considering the conservation of hydrocarbons on the surface in terms of the hydrocarbon concentration C_w, Guibert & Dicocco write that:

$$\frac{dC_w}{dt} = h_m\left(C_g - C_w\right) - \sigma\left(C_w, T_w\right), \qquad (10)$$

by assuming that the catalytic reaction rate is instantaneous. Since the hydrocarbons on the surface are consumed during operation, Guibert & Dicocco argue that C_w tends to zero and equation (10) can be expressed as

$$h_m C_g = \sigma\left(C_w, T_w\right), \qquad (11)$$

where

$$h_m = \frac{Sh\, D_h}{d_w} \qquad (12)$$

and

$$C_g = \rho_g \chi. \qquad (13)$$

Guibert & Dicocco express the molar fraction of hydrocarbon in terms of the air-to-fuel equivalence ratio

$$\chi = \frac{\phi}{\left(\phi + \gamma\right)} \qquad (14)$$

where γ is a constant defined as

$$\gamma = 4.76\left(x + \frac{y}{4}\right)$$

for a hydrocarbon molecule $C_x H_y$. It is noted that $\gamma = 59.5$ for octane (C_8H_{18}) and is larger for longer chain molecules.

The power generated by the catalytic reaction is:

$$P_R = \sigma\left(-\Delta H\right) A_w, \qquad (15)$$

which, substituting in equations (11)-(14), becomes

$$P_R = \beta\chi\left(\phi\right) \qquad (16)$$

with the constant β defined as

$$\beta = \pi l_w Sh \rho_g D_h \left(-\Delta H\right).$$

Hot-wire energy balance

Equations (1), (6), (9) and (16) therefore express the overall energy balance of the hot-wire in terms of the significant variables:

$$I^2 R_w = -\beta\chi\left(\phi\right) + \left(R_w - R_g\right) F\left(U\right) + k_1 \frac{dR_w}{dt} \qquad (17)$$

To a linear approximation, the voltage perturbation over the hot-wire is

$$e_w = \phi'\left(\frac{\partial E_w}{\partial \phi}\right)_{i=0} + i\left(\frac{\partial E_w}{\partial I}\right)_{\phi'=0}, \qquad (18)$$

where it is noted that Guibert & Dicocco's sensor operated under a constant cross-flow velocity $\bar{U}$, meaning that a velocity perturbation term does not appear in equation (18). Both partial derivatives on the right hand side of equation (18) are then evaluated from equation (17).

It is noted that the catalytic reaction has been modelled as instantaneous. This assumption is reasonable since the catalytic reaction rate is expected to be of order $10^{-9} s$ [5]. As is shown later in this paper, this time-scale is several orders of magnitude smaller than those associated with the hot-wire and related circuitry, meaning that it has negligible effect on the sensor's bandwidth.

It is also noted that radiative heat exchange is not included in equation (17). Giubert & Dicocco [3] found that this term is small compared to those included in the energy balance. Obviously, radiative exchange is effectively instantaneous, and so must also have negligible effect on any of the sensor dynamics of interest.

Evaluation of $\left(\partial E_w / \partial \phi\right)_{i=0}$

Using Ohm's law, it follows that

$$\left(\frac{\partial E_w}{\partial \phi}\right)_{i=0} = \bar{I}\left(\frac{\partial R_w}{\partial \phi}\right)_{i=0} = \bar{I}\left(\frac{r_w}{\phi'}\right)_{i=0} \qquad (19)$$

Replacing R_w and ϕ by their respective mean and perturbation quantities in equation (17) gives

$$\begin{aligned} I^2\left(\bar{R}_w + r_w\right) &= -\beta\chi\left(\bar{\phi} + \phi'\right) \\ &+ \left(\bar{R}_w + r_w - R_g\right) F\left(\bar{U}\right) + k_1 \frac{d}{dt}\left(\bar{R}_w + r_w\right). \end{aligned} \qquad (20)$$

It is noted that the function $\chi\left(\bar{\phi} + \phi'\right)$ is non-linear in ϕ' and that the accuracy of a given truncated series approximation for this function depends on the hydrocarbon under investigation via the term γ in equation (14). For example, Figure 2 shows a comparison between the analytic expression for χ with the simplest approximation from its binomial series expansion

$$\chi\left(\phi\right) = \frac{\bar{\phi} + \phi'}{\gamma}. \qquad (21)$$

This approximation is adequate for octane but clearly inadequate for methane. Indeed, the longer the hydrocarbon chain, the more accurate this approximation becomes since γ becomes larger. Equation (21) is therefore an acceptable approximation to equation (14) for octane and longer chain hydrocarbon molecules i.e. the main constituents of automotive and aircraft fuels. Importantly, acceptable approximations for χ can be found for methane and other short molecules by including terms with a linear dependence on ϕ' and higher powers of $\bar{\phi}$ and γ. This means that linear analysis is reasonable for any hydrocarbon of interest.

Retaining only the first order terms, the time average of equation (20) is

$$\bar{I}^2 \bar{R}_w = -\frac{\beta\bar{\phi}}{\gamma} + \left(\bar{R}_w - R_g\right) F\left(\bar{U}\right), \qquad (22)$$

and its fluctuating component is

$$I^2 r_w = -\frac{\beta\phi'}{\gamma} + r_w F\left(\bar{U}\right) + k_1 \frac{dr_w}{dt}. \qquad (23)$$

Expressing equation (23) using the Laplace transform variable s, the transfer function between the wire resistance $r_w(s)$ and the fluctuation in equivalence ratio $\phi'(s)$ is

$$\frac{r_w(s)}{\phi'(s)} = \frac{\beta}{\gamma\left[F\left(\bar{U}\right) - \bar{I}^2\right]\left(1 + T_w s\right)} \qquad (24)$$

with the hot-wire time constant

$$T_w = \frac{\bar{R}_w k_1}{\left[R_g F\left(\bar{U}\right) + \beta\chi\left(\bar{\phi}\right)\right]}. \qquad (25)$$

Substituting equation (24) and the expression for $\bar{I}$ in equation (22) into equation (19), it follows that

$$\left(\frac{\partial E_w}{\partial \phi}\right)_{i=0} = \frac{y}{\left(T_w s + 1\right)} \qquad (26)$$

where

$$y = \frac{\bar{R}_w \bar{I} \beta}{\left[R_g F\left(\bar{U}\right) + \beta\chi\left(\bar{\phi}\right)\right]}. \qquad (27)$$

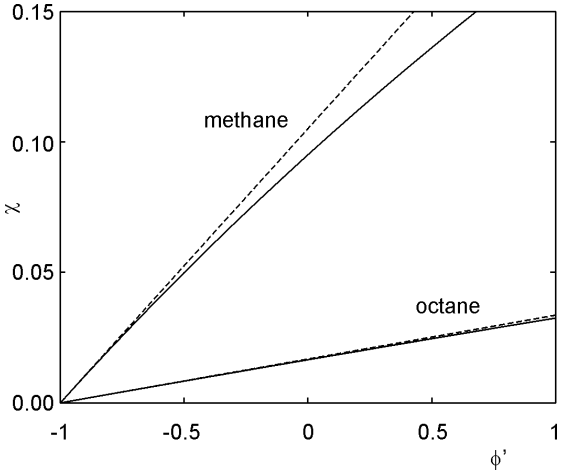

Figure 2: Exact (solid lines) and approximate (dashed lines) variation of χ with ϕ' for $\bar{\phi} = 1$

Evaluation of $\left(\partial E_w / \partial I\right)_{\phi'=0}$

The derivation of $\left(\partial E_w / \partial I\right)_{\phi'=0}$ involves similar working to that of $\left(\partial E_w / \partial \phi\right)_{i=0}$ presented above. Once again, using Ohm's law

$$\left(\frac{\partial E_w}{\partial I}\right)_{\phi'=0} = \bar{R}_w + \bar{I}\left(\frac{\partial R_w}{\partial I}\right)_{\phi'=0} = \bar{R}_w + \bar{I}\left(\frac{r_w}{i}\right)_{\phi'=0}. \qquad (28)$$

Analogous to equation (20), R_w and I are replaced by their respective mean and perturbation quantities in equation (17). Retaining only the first order terms, equation (22) is the time average of the resulting equation, with fluctuating component

$$2i\bar{R}_w \bar{I} = r_w\left[F\left(\bar{U}\right) - \bar{I}^2\right] + k_1 \frac{dr_w}{dt} \qquad (29)$$

Using Laplace transforms, it follows that

$$\frac{r_w(s)}{i(s)} = \frac{2\bar{R}_w \bar{I}}{\left[F\left(\bar{U}\right) - \bar{I}^2\right]\left(1 + T_w s\right)} \qquad (30)$$

where the hot-wire time constant T_w is defined in equation (25). Substituting equations (30) and (22) into equation (28) gives

$$\left(\frac{\partial E_w}{\partial I}\right)_{\phi'=0} = \bar{R}_w + \frac{\alpha}{\left(1 + T_w s\right)} \qquad (31)$$

where

$$\alpha = 2\bar{R}_w \left\{\frac{\bar{R}_w F\left(\bar{U}\right)}{\left[R_g F\left(\bar{U}\right) + \beta\chi\left(\bar{\phi}\right)\right]} - 1\right\}. \qquad (32)$$

Hot-wire transfer function

From equations (18), (26) and (31), the transfer function relating the hot-wire voltage perturbation to the equivalence ratio and hot-wire current perturbations is

$$e_w(s) = \frac{y}{\left(1 + T_w s\right)}\phi'(s) + \left[\bar{R}_w + \frac{\alpha}{\left(1 + T_w s\right)}\right] i(s) \qquad (33)$$

where the constants T_w, y and α are defined by equations (25), (27) and (32) respectively.

Feedback circuit and overall transfer function

Figure 3 shows the hot-wire feedback circuit used by Perry [7]. The hot-wire resistance is in series with an inductance L_w, which arises from the leads connecting the hot-wire to the bridge. Perry [7] shows that this inductance, and the balance inductance L_b, must be modelled in order to model the often observed oscillation and instability of hot-wire feedback circuits.

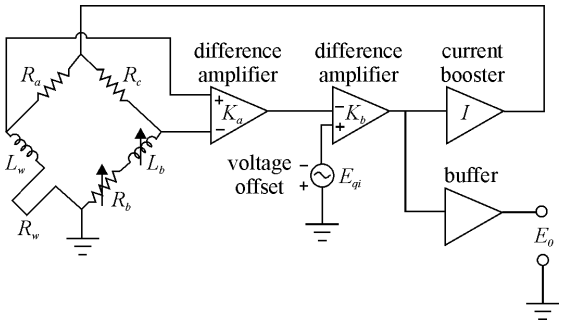

Figure 3: Perry's [7] hot-wire feedback circuit

Elementary circuit analysis with ideal amplifiers gives the following relations between the perturbation variables

$$e_0 = \left(R_a + L_w s\right) i_1 + e_w, \quad (34)$$

$$e_0 = \left(R_c + R_b + L_b s\right) i_2, \quad (35)$$

and

$$e_0 = K e_i = K\left(R_a i_1 - R_c i_2\right) \quad (36)$$

where

$$K = K_a K_b.$$

The transfer function between ϕ' and e_0 resulting from a linearised approximation to the combination of equation (33) with equations (34)-(36) has three poles and a single zero. However, Perry [7] shows that if one of these poles and the zero are far enough into the left half-plane, they have negligible effect on the dynamics of the feedback circuit. This is the case in the present investigation, and the overall transfer function can be approximated by a second order system defined as

$$\frac{e_0}{\phi'} = \frac{-K_1}{\left(T^2 s^2 + 2\xi T s + 1\right)} \quad (37)$$

where the sensitivity is

$$K_1 = \frac{K R_a \left(R_b + R_c\right) y}{\left(R_b + R_c\right)\left(R_a + \bar{R}_w + \alpha\right) + K\left(\hat{R} + R_c \alpha\right)}, \quad (38)$$

with

$$\hat{R} = R_w R_c - R_a R_b.$$

The undamped natural frequency ω_n of the circuit is the reciprocal of T, which is defined as

$$T^2 = \frac{K R_c L T_w}{\left(R_b + R_c\right)\left(R_a + \bar{R}_w + \alpha\right) + K\left(\hat{R} + R_c \alpha\right)} \quad (39)$$

with

$$L = L_w - \frac{R_a}{R_c} L_b.$$

Finally,

$$2\xi T = \frac{\left[\left(R_a + R_w\right)\left(R_b + R_c\right) + K\hat{R}\right] T_w}{\left(R_b + R_c\right)\left(R_a + \bar{R}_w + \alpha\right) + K\left(\hat{R} + R_c \alpha\right)}, \quad (40)$$

which completes the model of the constant temperature hot-wire sensor incorporated into the feedback circuit.

DISCUSSION

Frequency response of hot-wire

As was the case for constant temperature anemometry [7], equation (26) shows that the lumped body representation of the hot-wire results in a first order transfer function between the hot-wire voltage and the equivalence ratio. Equation (31) shows that this is also the case for the transfer function between the hot-wire voltage and the hot-wire current. The hot-wire time constant T_w is the same for both transfer functions and the terms β and χ quantify the effect of the catalysis on the hot-wire.

The frequency response of the hot-wire can be estimated by using physically sensible values for each of the terms in equation (26). This paper assumes the following: i) the specific heat capacity of the hot-wire c is $2.86\ MJ/m^3$ [4], ii) the hot-wire resistivity is $10^{-8}\ \Omega m$ [4], iii) the sensitivity of hot-wire's resistance to temperature variations a is $3.5\times10^{-3}\ 1/K$ [7] and iv) the hydrocarbon diffusion coefficient D_h is $10^{-5}\ m^2/s$ [4]. Guibert & Dicocco [3] used a hot-wire of length l_w of $3mm$ to study octane fuel. Their sensor shown in Figure 1 had a Reynolds number based on hot-wire diameter of 15 and, it is assumed, a Prandtl number of 0.7. With the hot-wire heated to $950K$, which was above the experimentally observed self-ignition temperature of stoiciometric octane, the above parameters give a mean resistance $\bar{R}_w$ of $0.572\ \Omega$ for their $15\mu m$ hot-wire. Most importantly, the hot-wire's time constant is $0.00241\ s$, meaning that its roll-off frequency is $66\ Hz$, and its sensitivity y is $0.183\ V$.

The resulting transfer function given by equation (26) is shown in Figure 4 for both the $15\mu m$ and $5\mu m$ hot-wires. As expected, the smaller diameter hot-wire has a broader bandwidth, due mainly to its smaller volume. The smaller diameter wire is also more sensitive primarily because of the relative scaling of the hot-wire's volume and surface area with its diameter. Reducing the diameter reduces the total amount of energy released into the hot-wire by the catalytic reaction because the hot-wire's surface area is reduced. However, the thermal capacity of the hot-wire is reduced by a greater degree because it is dependent on the hot-wire's volume.

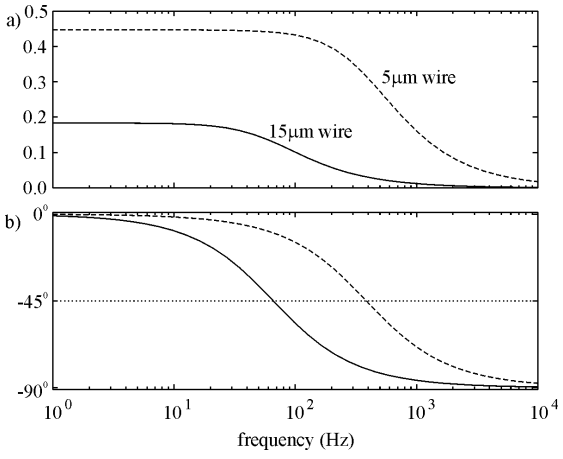

Figure 4: a) Amplitude and b) phase response of hot-wire voltage to fluctuations in equivalence ratio

It is also noted that the phase in Figure 4 is always negative. This is the opposite to constant temperature anemometry, and can be understood by referring to the hot-wire's energy balance in

equation (17). Positive perturbations in velocity decrease the internal energy of the hot-wire since increased velocity increases the forced convection, whereas positive perturbations in equivalence ratio increase the hot-wire's internal energy. This negative phase relationship for the hot-wire transfer function carries through the rest of the analysis.

The expression for the hot-wire time constant given in equation (25) also shows that the catalysis marginally *increases* the hot-wire frequency response above that for constant temperature anemometry. Ignoring the catalysis on the $15\mu m$ hot-wire in the present case results in a roll-off frequency of approximately $49\ Hz$, as opposed to the calculated $66\ Hz$ response given above for the equivalence ratio sensor. It is emphasised, however, that this effect is not expected to be large. Equation (39) shows that the time constant of the bridge circuit, which is the reciprocal of the circuit's undamped natural frequency, is proportional to the square root of the hot-wire's time constant, rather than directly proportional.

Of course, the hot-wire's sensitivity and frequency response also depend on the hydrocarbon being sampled. Although not presented in this paper, preliminary calculations nonetheless suggest that the sensitivity varies by considerably less than an order of magnitude over the range of hydrocarbons of likely interest. More importantly, these calculations also suggest that the frequency response appears to increase with reduced hydrocarbon chain length, such that a methane sensor with the parameters listed earlier will have a roll-off frequency of roughly $145\ Hz$. This is considered to be a significant, and is worth investigating further experimentally.

Frequency response of feedback circuit

The transfer function relating the equivalence ratio perturbations to the bridge output voltage is given by equations (37) to (40). This is a second order system, and the circuit parameters listed in Table 1 were varied in order to achieve a damping ratio ξ of approximately 0.6, which gives a reasonably flat frequency response and acceptable step response. The resulting frequency responses of both the $15\mu m$ and $5\mu m$ hot-wires are shown in Figure 5.

The undamped natural frequencies of both wires can be seen in Figure 5 and are listed in Table 1. Based on the authors' experience with CTA, the calculated value of ω_n is reasonable for the $5\mu m$ hot-wire, suggesting that the calculation for the larger diameter wire is also reasonable. This thicker diameter hot-wire is studied by Guibert & Dicocco [3], and it has a bandwidth that is significantly higher than any equivalence ratio sensor known to the authors.

It should be noted that the reduced sensitivity of the bridge output voltage to equivalence ratio perturbations with the smaller diameter hot-wire is not due to the sensitivity of the hot-wire itself. As Figure 4 showed, the smaller hot-wire is more sensitive. Rather, the reduced sensitivity of the bridge output voltage arises from the choice of the resistances listed in Table 1. These values were chosen in order achieve the desired damping ratio of 0.6.

hot-wire diameter	$5\mu m$	$15\mu m$
K	1000	1000
$R_c\ (\Omega)$	1000	1000
$T_w\ (ms)$	0.41	2.41
$R_a\ (\Omega)$	100	100
$\bar{R}_w\ (\Omega)$	5.15	0.572
$R_g\ (\Omega)$	1.53	0.170
$L_w = L_b\ (\mu H)$	5	5
$R_b\ (\Omega)$	47.5	60
ξ	0.604	0.597
K_1	2.88	10.08
$\omega_n\ (Hz)$	14,882	1,970

Table 1: bridge circuit parameters used for the two hot-wire diameters studied

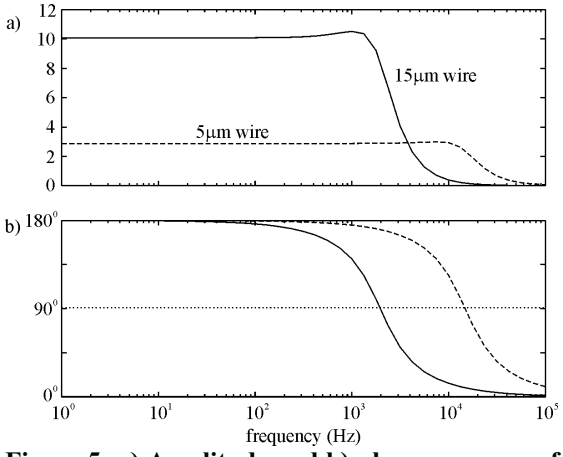

Figure 5: a) Amplitude and b) phase response of bridge output voltage to fluctuations in equivalence ratio

Finally, some mention should be made regarding the choice of hot-wire diameter, since it evidently has a large effect on the sensor's bandwidth. Recent discussions with Guibert [2] revealed that the use of their relatively thick $15\mu m$ hot-wire was necessitated by mechanical considerations. A hot-wire at $950K$ is significantly more likely to break than one operating at more typical overheat ratios. It must therefore be thicker,

especially given the relatively difficult operating environments in which this form of hot-wire sensor will most likely be used.

CONCLUSIONS

This paper presented a dynamic analysis of a fast response, air-to-fuel equivalence ratio sensor developed by Guibert & Dicocco [3]. This sensor utilises the operating principles of constant temperature hot-wire anemometry (CTA), with the hot-wire made from a catalytic material that is heated to a temperature above the ignition temperature of the fuel/air mixture. The wire therefore causes the mixture surrounding it to react and release energy to the wire, thus acting analogously to the forced convection sensing in CTA.

The $15\mu m$ diameter hot-wire used in Guibert & Dicocco's [3] study was calculated in this paper to have a bandwidth of $1{,}970Hz$. By reducing the sensor diameter to $5\mu m$, the calculated bandwidth increased to $14{,}882Hz$, although the high overheat temperature of the sensor and its likely challenging operating environments are expected to preclude hot-wires as thin as this. Nonetheless, the thicker diameter hot-wire studied by Guibert & Dicocco [3] is calculated to have a bandwidth that is significantly higher than any equivalence ratio sensor known to the authors.

ACKNOWLEDGMENTS

The authors would like to express their gratitude to the late Prof. Tony Perry, without whose inspirational teaching and scholarship, this paper would not have been conceived, let alone written.

REFERENCES

1. Blackwelder, R.F., 1981, "Hot-wire and hot-film anemometers", in Methods of Experimental Physics: Fluid Dynamics, part A, vol. 18, pg. 259-315
2. Guibert, P., 2002, private communication
3. Guibert, P. & Dicocco, E., 2002, "Development of a local continuous sampling probe for the equivalence air-fuel ratio measurement. Application to spark ignition engine", Experiments in Fluids, vol. 32, pg. 494-505
4. Incropera, F.P. & De Witt, D.P., 1990, "Fundamentals of heat and mass transfer", 3th edition, John Wiley
5. Kohse-Hoinghaus, K.. & Jeffries, J.B. (eds.), 2002, "Applied combustion diagnostics", Taylor & Francis
6. Kramers, 1946, "Heat transfer from spheres to flowing media", Physics, vol. 12, pg. 61-80
7. Perry, A.E., 1982, "Hot-wire anemometry", Clarendon Press, Oxford